



**HAL**  
open science

# Experimental investigation of the laminar – Turbulent transition and crossflow instability of an oscillating airfoil in low speed flow

Arnaud Lepage, Yannick Amosse, Jean-Philippe Brazier, Maxime Forte,  
Olivier Vermeersch, Cedric Liauzun

## ► To cite this version:

Arnaud Lepage, Yannick Amosse, Jean-Philippe Brazier, Maxime Forte, Olivier Vermeersch, et al.. Experimental investigation of the laminar – Turbulent transition and crossflow instability of an oscillating airfoil in low speed flow. IFASD 2019, Jun 2019, Savannah, United States. hal-02613018

**HAL Id: hal-02613018**

**<https://hal.science/hal-02613018>**

Submitted on 19 May 2020

**HAL** is a multi-disciplinary open access archive for the deposit and dissemination of scientific research documents, whether they are published or not. The documents may come from teaching and research institutions in France or abroad, or from public or private research centers.

L'archive ouverte pluridisciplinaire **HAL**, est destinée au dépôt et à la diffusion de documents scientifiques de niveau recherche, publiés ou non, émanant des établissements d'enseignement et de recherche français ou étrangers, des laboratoires publics ou privés.

## EXPERIMENTAL INVESTIGATION OF THE LAMINAR – TURBULENT TRANSITION AND CROSSFLOW INSTABILITY OF AN OSCILLATING AIRFOIL IN LOW SPEED FLOW

A. Lepage<sup>1</sup>, Y. Amosse<sup>1</sup>, J.P. Brazier<sup>2</sup>, M. Forte<sup>2</sup>, O. Vermeersch<sup>2</sup>, and C. Liauzun<sup>1</sup>

<sup>1</sup> ONERA, the French Aerospace Lab – Châtillon Center  
Aerodynamics Aeroelasticity Acoustics Department  
29 avenue de la Division Leclerc, 92320 Châtillon, France  
arnaud.lepage@onera.fr,  
yannick.amosse@onera.fr,  
cedric.liauzun@onera.fr

<sup>2</sup> ONERA, the French Aerospace Lab – Toulouse Center  
Multi-Physics Department for Energy  
2 avenue Edouard Belin, 31400 Toulouse, France  
jean-philippe.brazier@onera.fr,  
maxime.forte@onera.fr,  
olivier.vermeersch@onera.fr

**Keywords:** Laminar-turbulent transition, wind tunnel tests, crossflow instability, aeroelasticity

**Abstract:** The transition from laminar to turbulent boundary layer has been largely investigated in the literature on the experimental side as well as on the numerical side but the processes specifically involved in both transitional and unsteady flows (unsteady aerodynamic or aeroelasticity) have to be studied more in details.

This paper describes an experimental investigation achieved through a wind tunnel test of an oscillating swept wing in low speed range. In order to force the apparition of Cross Flow instabilities, the model was installed with a 60° sweep angle under favorable pressure gradient ensuring the absence of Tollmien Schlichting instabilities. The model was equipped with hot-film sensors to estimate the laminar or turbulent state of the boundary layer through the measurement of wall shear stress. The synchronous acquisition of dynamic motion and hot-film signals allowed to analyse the unsteady effects on the Cross Flow induced transition. The wind tunnel test program was achieved following a parametric approach through the variation of significant parameters: the amplitude and frequency of the dynamic actuation, the flow speed velocity and the mean value of the airfoil angle of attack. The paper describes the main insights of the test campaign and the associated database and presents how the test setup provided a well-adapted mean to study dynamic motions of the transition location. In comparison to steady configuration, the transition was not located at a fixed chordwise position but covered an area with an intermediary state of the boundary layer between the laminar and turbulent states. Several tools and post processing methods were specifically tuned to calculate quantities of the transition position (time resolved signal, mean properties through a phase averaging process, intermittency ratio) in addition to classical time and frequency analyses. One of the main outcomes pointed out the mean location of the laminar – turbulent transition was weakly influenced by unsteady motion. The general trend indicated a

more upstream location of few percent in chordwise in comparison to the steady case without any motion.

The experimental results constitute a first step in the understanding of the interaction of Cross Flow instabilities and dynamic motion and in the assessment of ONERA modelling and numerical simulation capabilities.

## 1 INTRODUCTION

The introduction of green technology into aviation is essential to make major steps towards the environmental goals sets by ACARE (Advisory Council for Aeronautics Research in Europe) to be reached in 2050 within the objective of pollutant emissions reduction. In order to reduce fuel consumption levels, one of the technology keys of current European research programs such as Cleans Sky 2 [1] is the drag reduction using wing laminarity. The future generation of laminar transport aircraft concept generally relies on the design of high aspect ratio wings to improve its aerodynamic efficiency but leads to increase the wing flexibility. Significant fluid-structure interactions are expected during flight conditions and can result on one hand in adverse aerodynamics performances of the aircraft (drag increase) and on the other hand in degradation of the structural behavior (vibration comfort loss) [2]. Recent works pointed out the risk of aeroelastic instabilities of laminar wing on transport aircraft in comparison to fully turbulent wing (flutter margin decrease) [3].

The transition from laminar to turbulent boundary layer has been largely investigated in the literature on the experimental side as well as on the numerical side on airfoil or swept wing cases for steady or quasi-steady configurations [4] [5] [6]. But considering these studies, the mechanisms involved in both transitional and unsteady flows have to be studied more in details (especially in presence of unsteady aerodynamic or aeroelastic phenomena). Progress in Computational Fluid Dynamics improve continuously the fidelity level of the predictions for transitional flows but only the steady transition is taken into account in the design and simulation processes. Prediction tools suffer from a lack of validated transition and turbulence models for transitional and unsteady flows. At the same time, few experimental investigations are reported for the measurement of unsteady transition [7]. Some works have been published [8] [9] [10] [11] and typically referred to an oscillating airfoil case (2D configuration) which has practical applications to helicopter rotor blades, wind turbines and engine compressor blades. Experiments mainly focused on the dynamic stall phenomenon through the investigation of the state of the unsteady boundary layer (detection of flow transition, separation and reattachment) of a dynamically pitching airfoil. For fixed wing airplanes, there are several instabilities and transition mechanisms observed on a wing such as Tollmien-Schlichting (TS) instability, Cross Flow (CF) instability or attachment-line instability (sometimes referred as Görtler-Hämmerlin instability). The scope of work described in the paper is focused on the analysis of CF instabilities in the low speed range through a Wind Tunnel (WT) test on a swept wing. The objectives of this study are to examine the state of the unsteady boundary layer developed on the upper side of an ONERA-D airfoil model installed in 2.5D configuration and sinusoidally oscillated. The presented results provide insights into the influence of dynamic oscillation parameters on the transition location characteristics.

The first experiment is a first step of an ONERA roadmap based on several WT campaigns to improve the understanding of transitional and unsteady flows and to dispose of databases for the calibration of modelling and numerical simulation capabilities.

## 2 DESCRIPTION OF THE EXPERIMENTS

### 2.1 Experimental test setup

The WT test campaign was achieved in the TRIN1 research wind tunnel facility located in the ONERA Toulouse Center. This facility is an open return wind tunnel with a 0.35m x 0.6 m x 2m test section, operating at low speed [10-80] m/s and at atmospheric stagnation pressure and temperature. The low values of turbulence and noise levels of this facility are well adapted for the study of transition detection and instabilities analysis. The model was based on the symmetrical ONERA-D airfoil, which has already been used for several numerical and experimental investigations of transition phenomenon [12] [13] [14]. The model is composed of an intern aluminum frame and two resin skins, and had a 0.35m chord length and a 2m span. In order to force the apparition of CF instabilities, the model was installed with a 60° sweep angle. An overview of the experimental setup installed in the TRIN1 WT facility is illustrated in Figure 1.

The question of interaction between flows around the airfoil and wind tunnel side walls was raised, especially as the model is installed in 2.5D configuration from one wall of the test section to the opposite one with a sweep angle. In the walls-wing junction, the conflict between motion and airtightness is a classical issue for dynamic tests. Therefore, foams have been added at each wing root to limit air leakage minimizing friction or damping phenomena. Moreover, the test section of the TRIN1 facility is installed in an airtight cover chamber ensuring a low difference between plenum chamber and test section steady pressures.

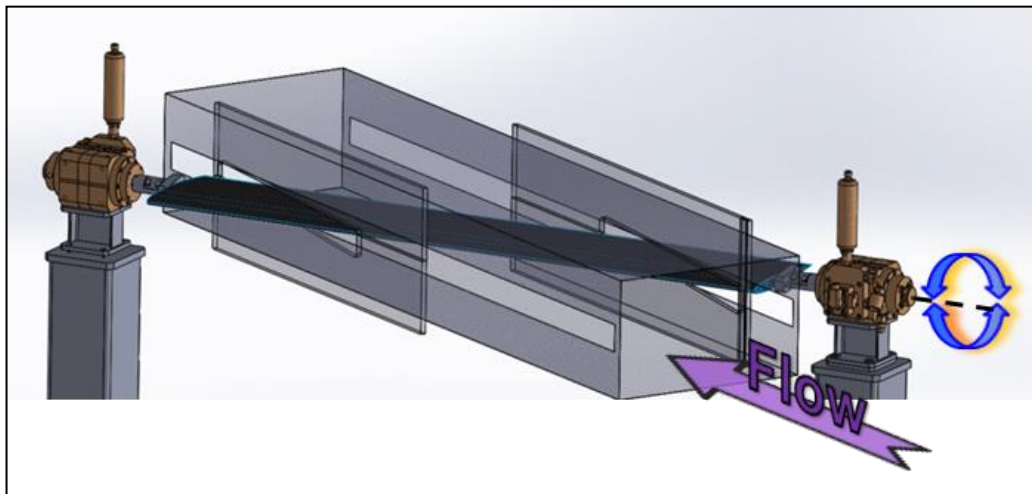


Figure 1: Illustration of the model installed in the WT test section.

The actuation of the wing was performed synchronously on each side by a “high torque - high speed” actuator composed of a rotary hydraulic jack operating at 200 bar using a fast response servo valve and a rotary potentiometer sensor (Figure 2). The actuation device includes a security system that prevented any unwanted torsional deformation of the airfoil. The wing pitch axis was located at mid-chord and the dynamic oscillation was driven by sinusoidal command signal defining the instantaneous angle of attack:

$$\alpha(t) = \alpha_0 + \Delta\alpha * \sin(2\pi f t) \quad (1)$$

where  $\alpha_0$  is the mean angle of attack,  $f$  and  $\Delta\alpha$  are the frequency and amplitude of the dynamic pitch motions.

Preliminary to the wind tunnel tests, the complete experimental setup was qualified under laboratory conditions to identify the dynamic behavior and to tune precisely the position feedback control laws.

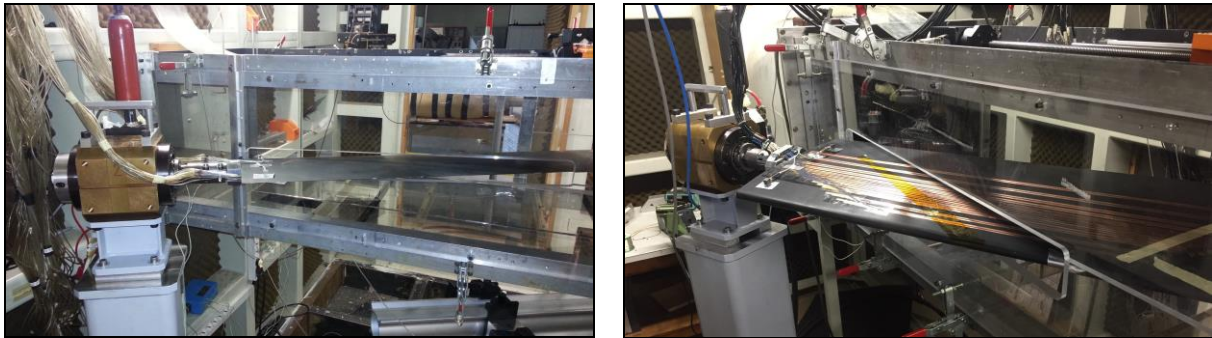


Figure 2: The WT test setup in the TRIN1 facility: Left and Right parts for actuation

Performances of the dynamic oscillation of the model were assessed by estimating the Frequency Response Function of the position sensors relatively to command signal. Actuation bandwidth is an important consideration and the goal was to cover the widest frequency bandwidth achievable by the experimental setup. Despite the individual performances of each actuator, the whole setup performances were restricted to a frequency bandwidth not exceeding 35 Hz. The presence of flexible structural modes at high frequency considerably altered the stability of the closed loop system. The synchronous dynamic functioning of the two actuators was validated in terms of phase and amplitude over the frequency bandwidth, as detailed in table 1.

Table 1: Dynamic performances of the experimental setup

Command Frequency (Hz)	Command amplitude (°)	Rotative Position 1 (°)	Rotative Position 2 (°)
5	5	5,02	5,01
10	3	3,03	3,01
15	2	2,04	2,02
25	1,5	1,56	1,52
35	1	1,08	1,03

The main output of the laboratory tests states that the experimental test setup fully filled the requirements and specifications of the WT tests:

- for the frequency parameter, a dimensionless analysis based on the reduced frequency ( $k = 2 * \pi * c / V_{\infty}$  for a streamwise chord length  $c = 0.7\text{m}$  and free stream velocity  $V_{\infty} = 70 \text{ m/s}$ ) indicated the frequency bandwidth is relevant for aeroelastic investigations (regarding the frequencies of the first structural flexible modes of large airplane flying in cruise conditions).
- for the amplitude parameter, previous studies [13] on the ONERA-D airfoil (steady case) pointed that the range of angle of attack variation was sufficient to induce significant motion of transition location.

## 2.2 Model instrumentation

In order to investigate the unsteady motion effects on the laminar-turbulent transition, the model was equipped with accelerometers and displacement sensors to measure the wing oscillations and hot-film sensors (Dantec 55R47) located on the upper surface to qualify the

state of the boundary layer. A schematic overview of the sensors arrangement can be found in Figure 3. In order to characterize the transition, the model was equipped with a limited number of hot-film sensors (12) but “optimally located” on the upper side between 10% and 60% chord length and arranged with an angle of  $30^\circ$  (with respect to y direction) to prevent disturbances and interferences between sensors. To precisely capture the transition, the sensors spacing was reduced to 2% chord length in the area of interest. Hot-films are heated by using home-made Constant Temperature Anemometers with an overheat ratio of 1.5. No calibration of the hot-film sensors was performed since the test objective was focused on the qualitative investigation of the boundary layer laminar or turbulent state. As in other studies [8], since the amplitude of the wall shear-stress fluctuations is much higher for turbulent boundary layers than laminar ones, the voltage output of each hot-film sensor provided a direct identification of the state of the boundary layer over it. Preliminary tuning was performed to adjust conditioning gains so that hot-film signals had similar magnitude.

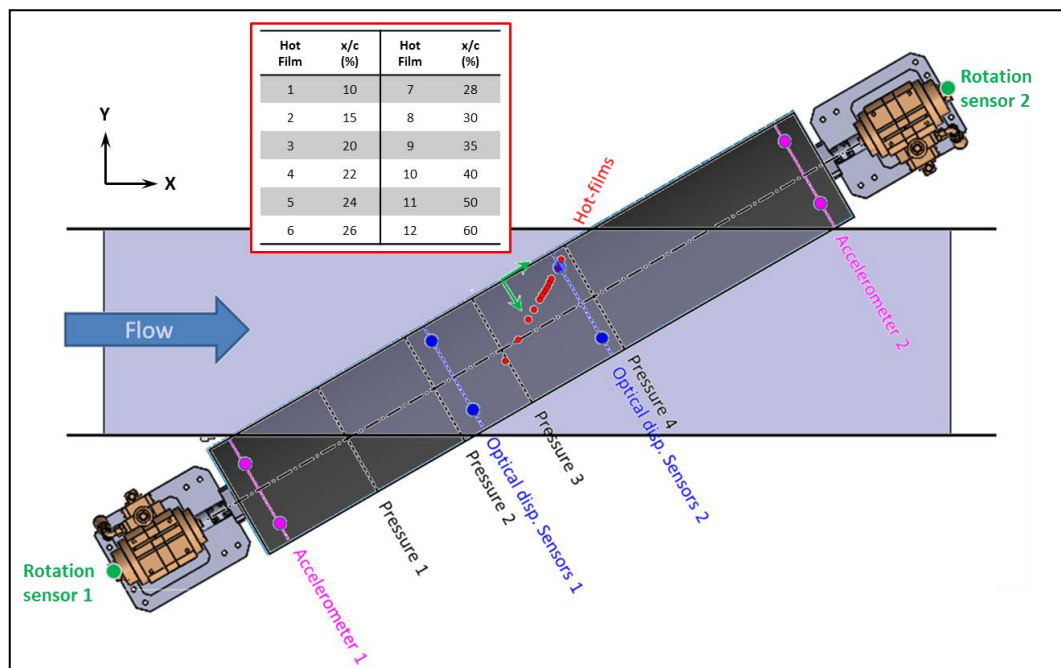


Figure 3: Overview of the model instrumentation

All unsteady signals (hot-film sensors, accelerometers, optical sensors and actuation rotation sensors) were recorded synchronously with a data acquisition system including a 24 bit Analog to Digital conversion per channel. Unsteady signals were sampled at a fixed rate of 20480 Hz.

The model was equipped with pressure taps to measure the steady pressure distributions in several sections. Pressure data are not presented in the paper but were used for comparison with exiting experimental databases [13] [14] and for correlation with numerical simulations.

### 2.3 Test program and aerodynamic conditions

The choice has been made to focus on the main case with an inflow velocity of 70 m/s corresponding to streamwise chord Reynolds number of  $3.14 \cdot 10^6$  and a mean angle of attack  $\alpha = -8^\circ$ . This value was selected to obtain a favorable pressure gradient on the upper side of the model ensuring the absence of TS instabilities and the apparition of Cross Flow instabilities.

The wind tunnel tests campaign was achieved following a parametric approach around this steady central case through the variation of the significant parameters:

- The frequency of the dynamic oscillation in the range [1 ; 35] Hz,
- The amplitude of the dynamic oscillation in the range of  $\pm 1^\circ$  to  $\pm 3^\circ$  (depending on the command frequency),
- The flow velocity in the range [30 ; 70] m/s,
- The value of the mean angle of attack in the range  $[-3^\circ; -13^\circ]$ .

As a preliminary first step in the investigation of dynamic motion effects on the transition, one of the main assumptions in the presented work and analysis, is that the flow and thus the transition mechanism remain unchanged in the spanwise direction (2.5D assumption) except in the vicinity of the test section walls.

### 3 EXPERIMENTAL RESULTS ON STEADY CASES

#### 3.1 Hot-film measurements

Before the investigation of unsteady effects on the transition, tests have been achieved to characterize the behavior of (classical) steady cases. Figure 4 represents the typical hot-film signals for the reference steady case  $\alpha_0 = -8^\circ$ ,  $V = 70\text{m/s}$ . The first hot-film signals present low output levels indicating that the boundary layer is laminar. Then turbulent burst can be observed on downstream chordwise locations sensors as the boundary layer begins to become unstable. The fully turbulent state is finally reached and characterized by a “broadband frequency noise” pattern.

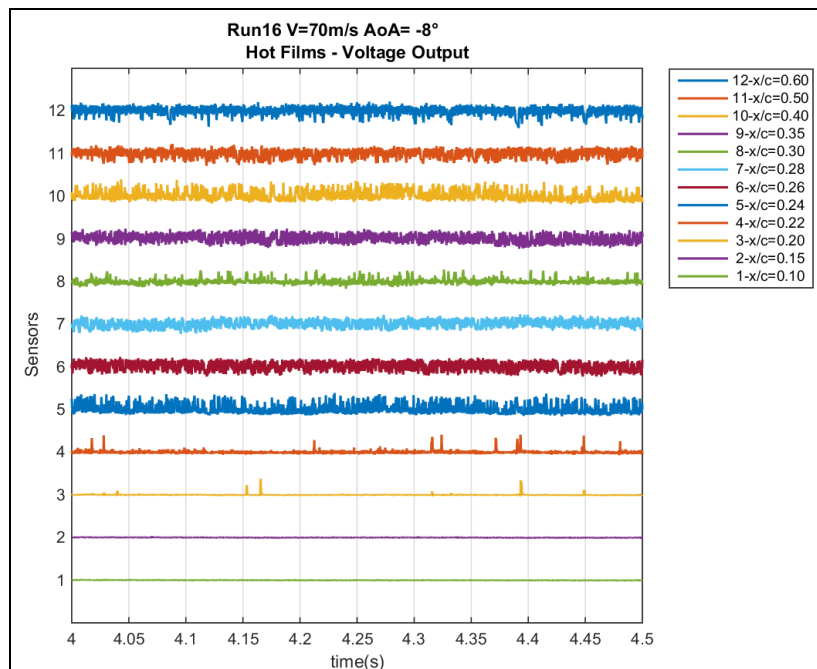


Figure 4: Time traces of the motion and hot film signals for a steady state

In order to qualify the boundary layer state, the hot-film signals are usually analysed using different statistical quantities such as Root Mean Square (RMS) or Skewness. The RMS distribution for the main case ( $\alpha_0 = -8^\circ$ ,  $V = 70\text{m/s}$ ) is shown in Figure 5 and provides the mean fluctuation amplitude of the wall shear stress at the sensor locations. The laminar flow over

the first part of the measurement area is represented by a low RMS level. The increase of RMS values with the highest levels of local fluctuations indicates the transitional region to reach the turbulent state characterized by high RMS values.

### 3.2 Transition location detection

The accurate definition of the transition location is a very complex process that can be based on the analysed statistical quantities (data type, maximum value, threshold value, intermittence value ...). In order to dispose of a “more systematic approach”, a methodology for the detection of the transition location has been proposed and relies on the calculation of the gradient of RMS distribution as shown in Figure 6. The selection of the maximum value of the gradient and adjacent points allows through a parabolic interpolation method to identify the transition point. For reference steady case, this methodology exhibits a transition located at 22.5% of the chord length in accordance with the hot-film temporal signals presented in Figure 5 suggesting a transition location between the sensors located at 22% and 24%.

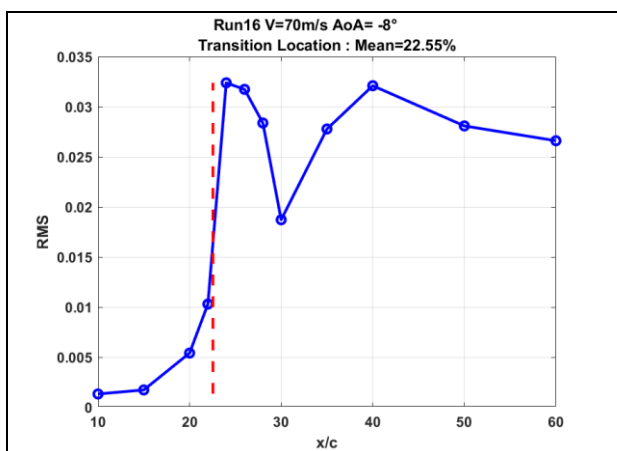


Figure 5: Chordwise Distribution of RMS values of hot-film signals

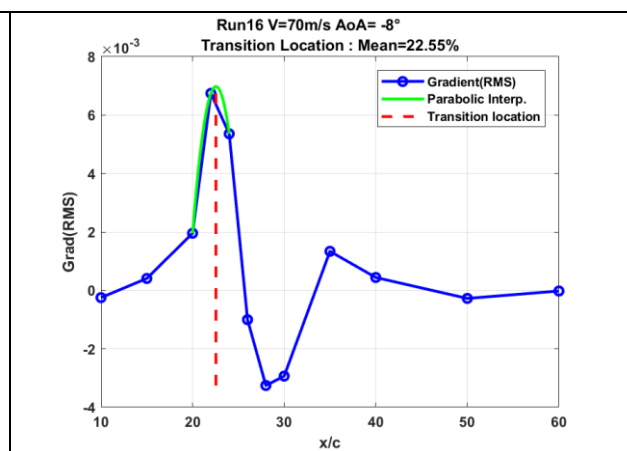


Figure 6: Automatic identification of the transition location based on the gradient of the RMS distribution of hot-film signals

The relevance of the proposed methodology is strongly dependent on the size of the transitional region, the spacing between the sensors, the selection criterion (maximum value, threshold value ...). Despite the risk of bias introduction, the main advantages are that the methodology can be used for both steady and unsteady tests and is very simple to implement for qualitative comparison between test points.

### 3.3 Spectral analysis

Additionally, spectral analysis of the hot-film signals also characterizes the boundary layer state and the frequency components of the instabilities. Spectral densities of the hot-film signals are presented in the Figure 7.

As reported in the literature [4] the CF instability mechanism exhibits stationary as well as traveling disturbances. The phenomena associated to the stationary waves are predominant in low turbulence environment and may result to the presence of micro roughness on aerodynamic surfaces. The stationary-vortex patterns are often visualized using sublimating chemical process or Infra-Red thermography. The existence of stationary CF for the considered test points has already been demonstrated [5] for identical test conditions. The unsteady CF can be directly extracted from hot-film measurements. As illustrated in Figure 7,

for the sensors located upstream the transition, high frequency components can be identified through the broad frequency bumps between 2 and 6 kHz and refer to the traveling waves.

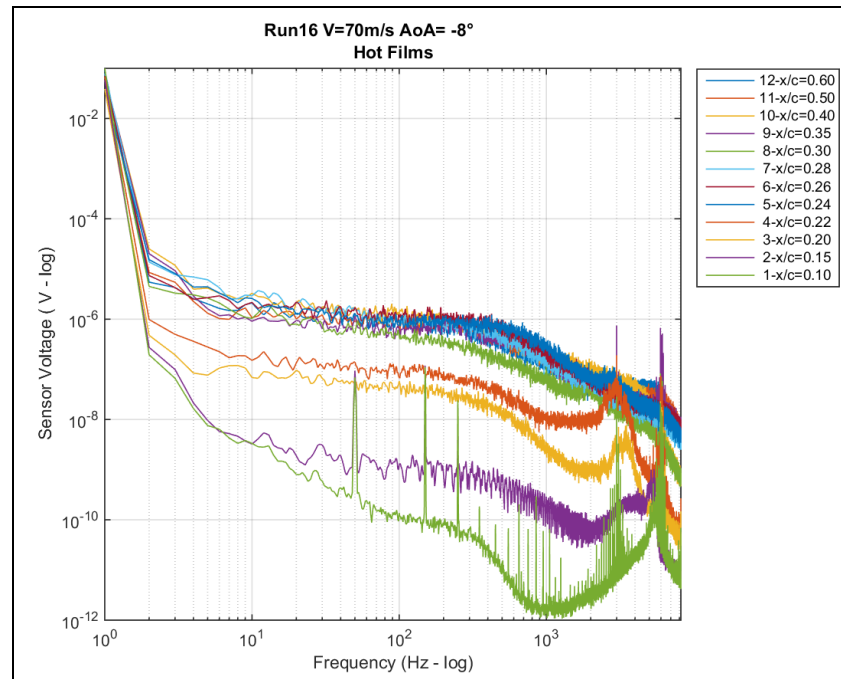


Figure 7: Spectral analysis of hot-film signals

It should be noticed that the sharp peak at 50 Hz is associated to the alternating current in France while the spectral lines at 3 and 6 kHz may correspond to the frequency of the wind tunnel fan and its first harmonics. Anti aliasing filters of the acquisition device were fixed at 8 kHz.

### 3.4 Stability analysis

Linear stability analysis has been conducted in order to estimate the range of unstable unsteady CF disturbances. First, boundary layer flow was computed based on experimental pressure coefficient measurements using the ONERA 3C3D boundary-layer code and the infinite swept wing assumption (2.5D configuration). Then, the stability of the boundary layer velocity profiles have been studied using linear local stability approach (Orr-Sommerfeld equation). The chordwise evolution of the obtained N-factors is plotted in Figure 8. The N factor represents the amplification of boundary layer instabilities: the higher the N factor is, the most amplified the instability is. Between 20 and 30% of chord, the frequency of the most amplified unsteady CF instability is around 2kHz which coincides with the observations of the spectral analysis of hot-film signals (Figure 7).

Transition is supposed to be triggered when the N-factor overcomes a given threshold  $N_T$ . Taking  $N_T=7$  as a critical value (which is a classical value for stability studies in this facility) provides a ‘numerical’ transition location at 23% of chord in close agreement with measurements.

Thus these calculations results clearly support the assumption that the investigated phenomena in the tested conditions (aerodynamic conditions, airfoil installation) are related to the laminar-turbulent transition driven by CF instabilities.

Previous [13] and present works have provided experimental database that demonstrated the existence of amplified disturbances in the boundary layer according to the CF scenario

(steady and unsteady CF instabilities). But considering the low frequency range of dynamic motion explored in this work, the analyses of the interactions between pitching oscillation and unsteady transition only concerned the steady CF instabilities.

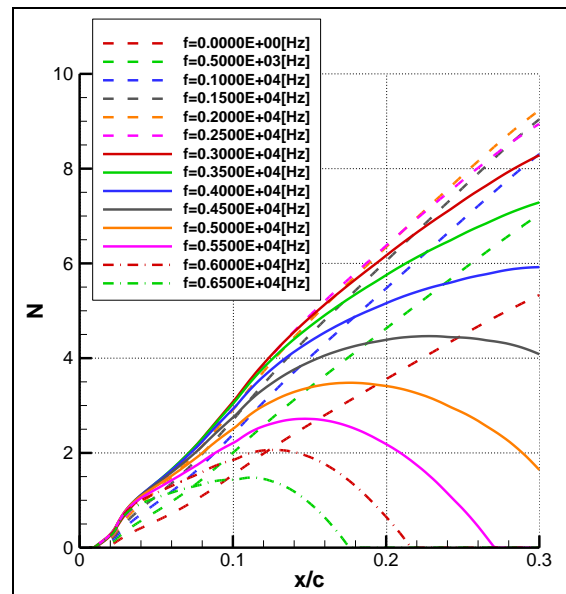


Figure 8: Stability analysis – Chordwise evolution of the N-factors

## 4 EXPERIMENTAL RESULTS WITH A DYNAMIC OSCILLATION

### 4.1 Hot film measurements for a dynamic case

In comparison to steady configuration, the transition was not located at a fixed chordwise position during a dynamic motion test but covered an area with an intermediary state of the boundary layer between the laminar and turbulent states. Figure 9 presents the hot-film signals recorded for dynamic oscillation with a frequency of 5 Hz and an amplitude of  $\pm 1^\circ$  around the steady case  $\alpha_0 = -8^\circ$  and  $V = 70 \text{ m/s}$ .

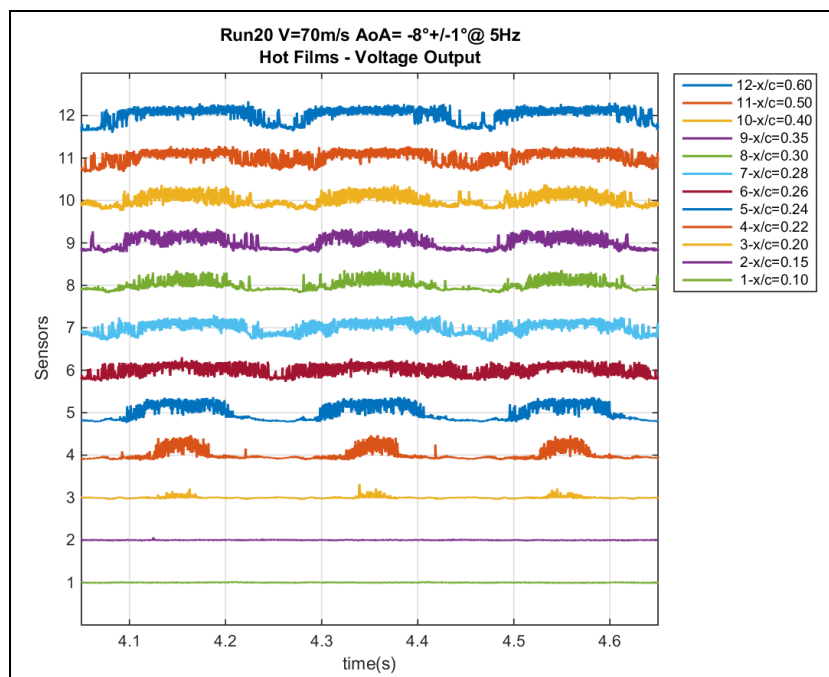


Figure 9: Time traces of the motion and hot film signals for a dynamic motion test point

The signals of the hot-film sensors #4 or #5 are typically representative of the effects of the unsteady transition position, alternating between two main states over the motion period. When the flow is laminar, the output voltage is characterized by a low mean value and a low level of fluctuations. These two quantities increase significantly as the wall shear stress rises in the boundary layer.

In order to analyse the motion effect, several tools and post processing have been specifically tuned to calculate specific quantities and are reported in the following section and illustrated for the test case presented in the section 4.1.

#### 4.2 “Time resolved method” for the estimation of the transition location

The method for the estimation of the transition location presented the section 3.2 has been adapted to the dynamic test point using a sliding window processing. The method consists in the calculation of the RMS distribution for hot-film data over a temporal block  $[t-\Delta t ; t+\Delta t]$ . Then the instantaneous transition location is identified through the methodology developed in the section 3.2 and based on the gradient of the RMS distribution. Time blocks are small regarding the dynamic pitching period and the processing is performed with overlapping to increase the temporal resolution of the “time resolved” transition location”.

The method was applied to a steady case ( $\alpha_0 = -8^\circ$ ,  $V = 70\text{m/s}$ , no motion) for validation. As presented in Figure 10, the time evolution of the transition location is obtained, its averaged value is 22.6% of chord length (similar to the result obtained in 3.2) and its standard deviation less than 0.5 % of chord length indicating clearly a stable and steady location of the transition.

Figure 11 presented the results obtained for a test point with similar aerodynamic conditions ( $\alpha_0 = -8^\circ$ ,  $V = 70\text{m/s}$ ) but for the case of pitch dynamic motion (oscillation of  $\Delta\alpha = \pm 1^\circ$  at  $f = 5\text{Hz}$  around the mean angle of attack  $\alpha_0 = -8^\circ$ )

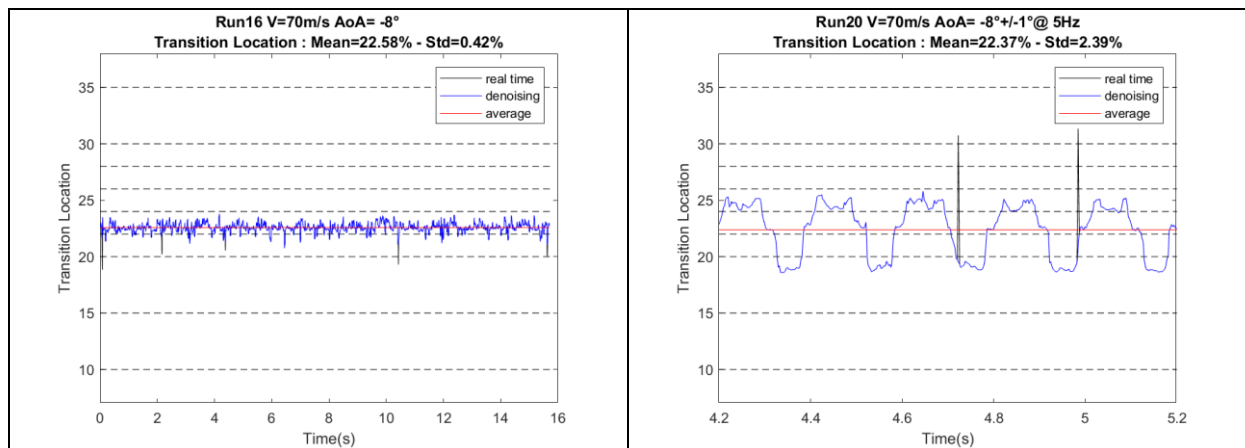


Figure 10: Time traces of the “instantaneous” Transition location for a steady test point

Figure 11: Time traces of the “instantaneous” Transition location for a dynamic test point

As expected, the transition location oscillates in the chordwise direction and is completely driven by the motion parameters, frequency and amplitude. The time trace of the position location is not a purely harmonic signal (w.r.t. to the sinusoidal motion command) which may result from limitations of the processing methodology as well as the presence of non linearities. The averaged value of the location signal is 22.4% of chord length and the dynamic fluctuations of the position are characterized by a standard deviation of about 2.4% of chord length.

### 4.3 “Phase averaged method” for the estimation of the transition location

In the second process, the period  $T$  of the airfoil motion was decomposed into  $N$  phases ( $N = 16$  classes – Figure 12), each phase referring to a specific block centered on a time  $t_k$  such that

$$T_k = (k-1) * T/N \text{ with } k = 1 \dots N \quad (2)$$

For each hot-film sensor, the signal was post processed according to the phasing process based on the separated classes. For each class, RMS calculations and transition location method described in 3.2 were used leading to the identification of the transition location over the dimensionless motion period illustrated in Figure 13 referring to the same test point ( $\alpha_0 = -8^\circ$ ,  $V=70\text{m/s}$ ,  $\Delta\alpha = +/- 1^\circ$  and  $f = 5\text{Hz}$ ).

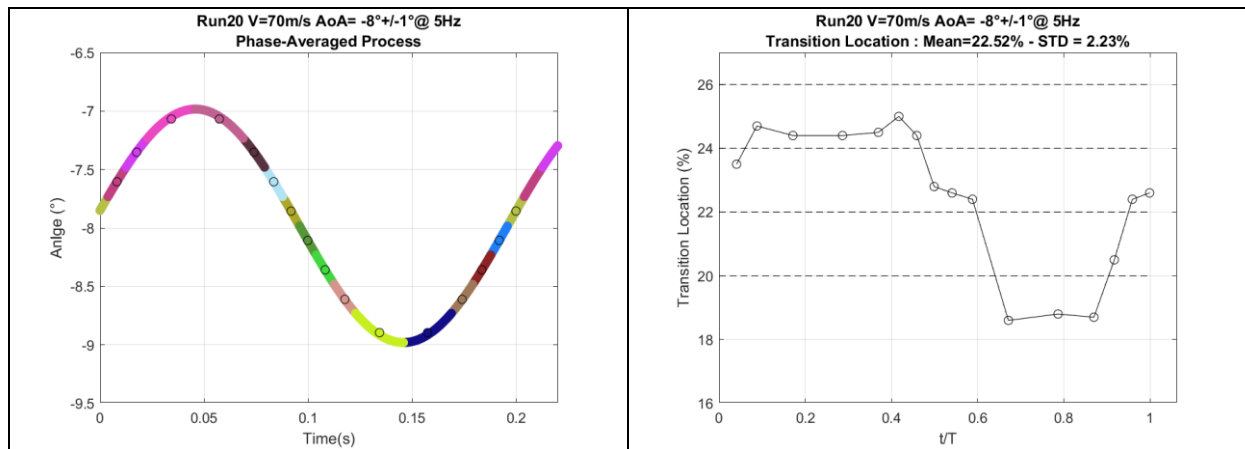


Figure 12: Phase-average method based on the pitching motion period

Figure 13: Phase-averaged transition location over the dimensionless motion period  $t/T$

The analysis of the results indicates an averaged value of 22.3 % of chord length and a level of dynamic fluctuations of 2.2 % of chord length which appear to be consistent with previous results.

### 4.4 “Intermittency factor method” for the estimation of the transition location

The last approach for the estimation of the transition location is based on the identification of the point with 50 % intermittency, where the boundary layer is intermittent between the laminar state and the turbulent regime. Each hot-film signal was post processed separately to estimate the laminar to turbulent ratio regarding the pitching period. The methodology has been implemented through a sliding window calculation to identify the threshold separating the two states. As illustrated in the Figure 14, the results are presented for the dynamic test point ( $\alpha_0 = -8^\circ$ ,  $V=70\text{m/s}$ ,  $\Delta\alpha = +/- 1^\circ$  and  $f = 5\text{Hz}$ ).

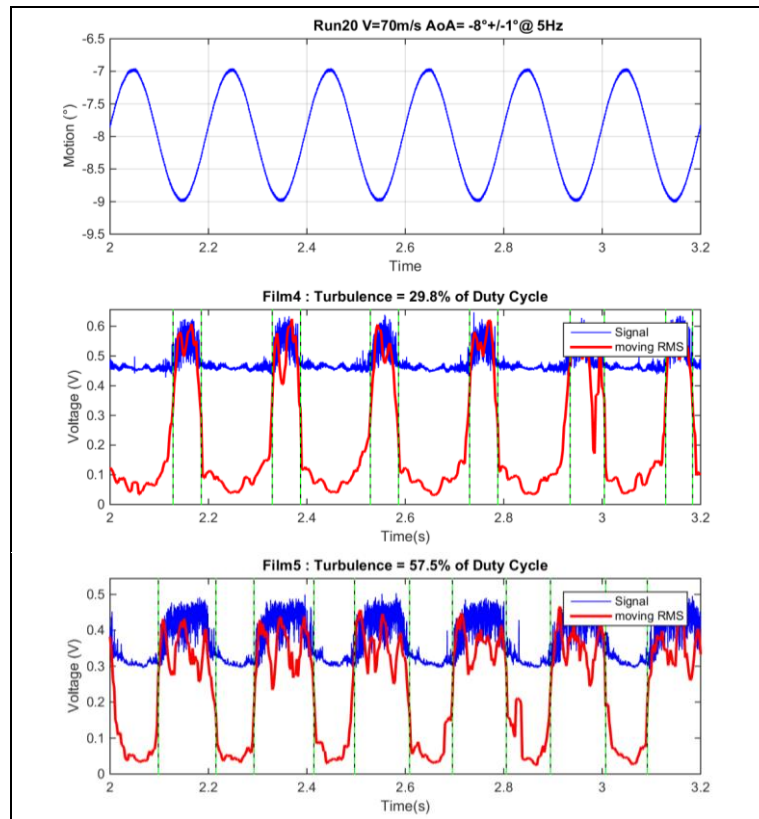


Figure 14: Estimation of the turbulent to laminar ratio

The analysis indicates the intermittency factor is equal to 29.8 % for the 4<sup>th</sup> hot-film (i.e. the percentage of the motion period corresponding to the turbulent state) and 57.5% for the 5<sup>th</sup> hot-film respectively located at 22% and 24% of chord length. Then a interpolation of the data provides a transition location of 23.5% corresponding to 50 % intermittency factor. By comparison with the previous method, this value is slightly higher.

## 5 DYNAMIC MOTION EFFECTS ON THE TRANSITION LOCATION

The effects of the amplitude and the frequency of the dynamic motion on the transition location are illustrated in Figure 15 & Figure 17, and Figure 16 & Figure 18, respectively. The main outcome of the analyses is that there is no strong interaction between the boundary layer state and the dynamic motion. Data obtained from the detection methods suggest, as presented in Figure 15, that the average transition location tends to be located “slightly” upstream in chordwise position in presence of dynamic motion: a more upstream location of few percent of chord length in comparison to the steady case. The results should be here considered with some caution since the minimum spatial discretization of hot-film sensors (2%) is the same order of magnitude than the observed phenomena. Moreover, the motion amplitude parameter acts as an amplification factor (Figure 15): the higher the motion amplitude, the more upstream transition location. Contrary to the amplitude, the frequency parameter does not seem to have any influence on the mean transition location (Figure 16) over the entire frequency bandwidth [1 - 35] Hz.

Figure 15 and Figure 16 also indicate that the outputs provided by the “intermittency factor” method are offset from the 2 others methods. This observation may result from the selected threshold or interpolation tool used in the method for the estimation of the laminar to turbulent ratio. Nevertheless the observed trend match very well with the other conclusions.

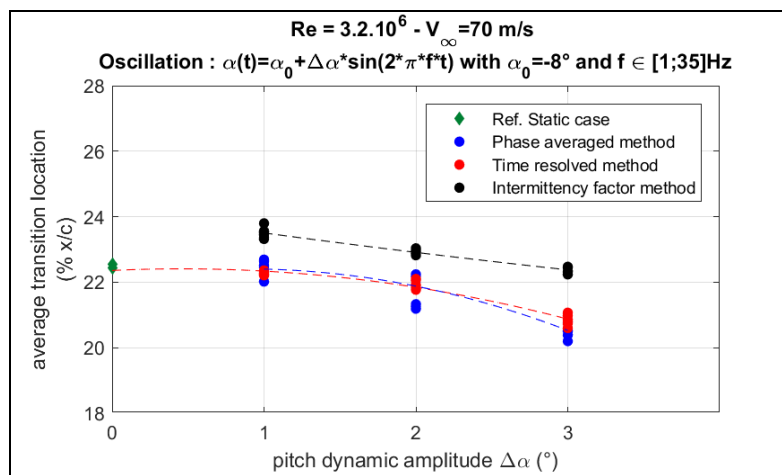


Figure 15: Influence of the pitch oscillation amplitude on the average transition location

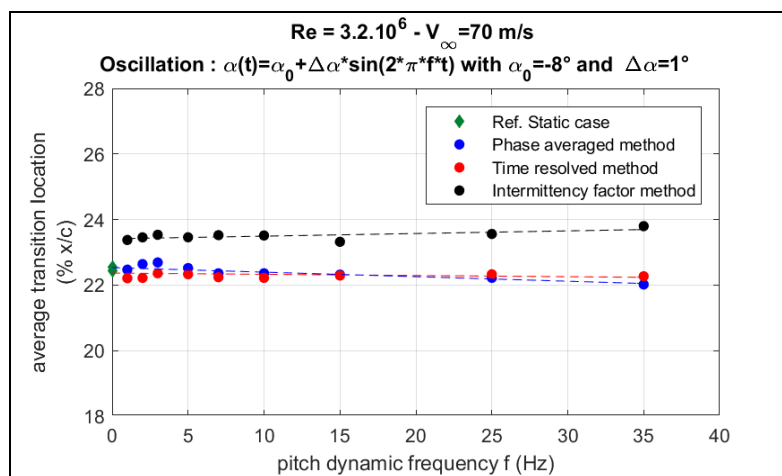


Figure 16: Influence of the pitch oscillation frequency on the average transition location

As for steady or quasi-steady cases, the oscillation amplitude (i.e. the unsteady angle of attack) completely drives the position envelop of the transition point. Figure 17 shows the motion amplitude quasi-linearly defines the size of the area with intermittent state of the boundary layer during the motion period. The RMS value of transition position varies proportionally to the amplitude of motion.

The frequency parameter appears to be less predominant. No peak or resonance phenomenon clearly emerges from the Figure 18, describing a flat evolution of the fluctuation levels of the transition location as a function of the frequency.

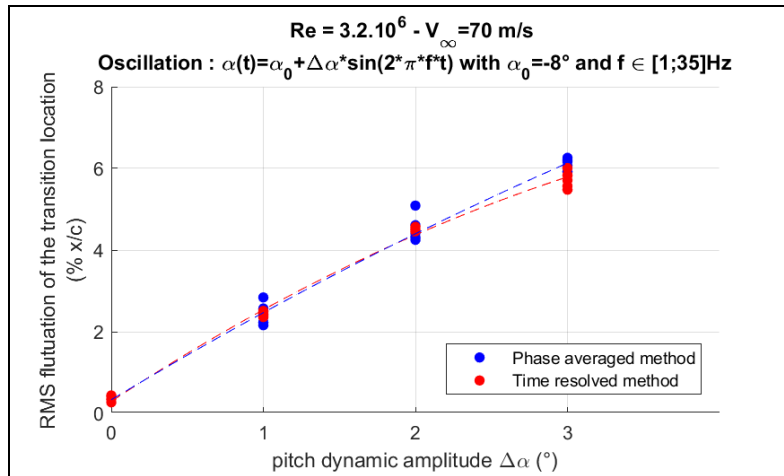


Figure 17: Influence of the pitch oscillation amplitude on the fluctuation levels of the transition location

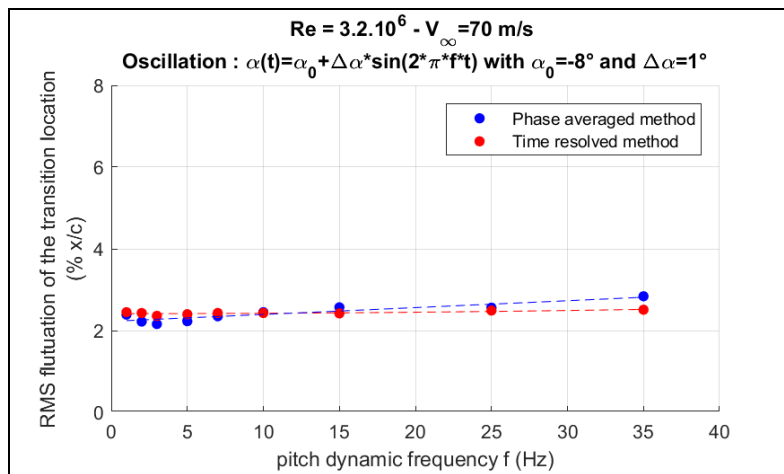


Figure 18: Influence of the pitch oscillation frequency on the fluctuation levels of the transition location

Therefore up to now, based on these analyses, no strong interaction can be noticed between the transition induced by CF instabilities and the dynamic motion of the wing. The only weak trend indicates that average transition location tends to be located more upstream than for the equivalent steady case. This insight should nevertheless be balanced with the assumptions and limitations of test setup and analysis methods and with the uncertainties mainly related to experimental meshing of hot-film sensors (number and spacing).

## 6 CONCLUSIONS AND WAY FORWARD

An experimental investigation of an oscillating wing has been conducted in the TRIN1 ONERA low speed facility to study the laminar-turbulent transition. The model was installed in a 2.5D configuration to analyse the apparition of Cross Flow instabilities and equipped with hot-film sensors to estimate the state of the boundary layer through the measurement of wall shear stress. The works presented in this paper allowed at first to assess the feasibility of operating a dynamic motion setup in a WT environment for transition investigation purpose. Then several tools and post processing methods were specifically developed to evaluate quantities related to the transition.

In comparison to (quasi) steady configuration, the dependence of the transition on the angle of attack was weakly influenced by unsteady motion. Database analyses pointed out a trend to observe a more upstream location of the average transition location in comparison to the steady case without any motion. Nevertheless, the scale of the phenomena should be carefully balanced with the uncertainties of the measurement and post-processing methodologies.

Numerical restitution of the experimental database have been recently performed [15] with the ONERA software elsA [16], simulating of the oscillating airfoil with free transition. Preliminary results confirm the trend of an average transition point located more upstream in chordwise direction.

This wind tunnel test constituted a preliminary step of ONERA investigations on the interactions between laminarity and aeroelasticity. These results have been obtained in incompressible flow in low speed. Further research needs to be conducted to consider compressible flow and large Reynolds number effects, to investigate several transition mechanisms (CF instabilities as well as the TS instabilities, boundary layer interaction with shock ...) while correlating simultaneously with unsteady loads on a movable/flexible model. A key long-term objective will be the investigation and characterization of flutter of a laminar wing on a realistic flexible model.

## 7 ACKNOWLEDGMENTS

The preliminary works and wind tunnel tests have been achieved within the frame of the ONERA's joint research project ARF TRAVELS. A part of the database analyses has been funded within the frame of the Joint Technology Initiative JTI Clean Sky 2, AIRFRAME Integrated Technology Demonstrator platform "AIRFRAME ITD" (contract N CSJU-CS2-GAM-AIR-2014-15-01 Annex 1, Issue B04, October 2nd, 2015) being part of the Horizon 2020 research and Innovation framework program of the European Commission.

## 8 REFERENCES

- [1] Cleansky 2 website : <http://www.cleansky.eu/>
- [2] Mabey D.G., Ashill P.R., Welsh B.L., (1987). Aeroelastic oscillations caused by transitional boundary layers and their attenuation. *Journal of Aircraft*, 24(7), 463-469.
- [3] Tichy L., Mai H., Fehrs M., Nitzsche J., Hebler A. (2017). Risk Analysis for Flutter of Laminar Wings, *IFASD 2017*, June 25-28, Como, Italy.
- [4] Course at Von Karman Institute for Fluid Dynamics, *Advances in Laminar-Turbulent Transition Modeling*, RTO-EN-AVT 151, 9-12 June 2008, Sint-Genesius-Rode, Belgium.

- [5] Arnal D., Coustols. E. and Juillen J. (1984). Experimental and Theoretical Studies of Boundary Layer Transition on a Swept Infinite Wing, *Laminar-Turbulent Transition Symposium*, July 9–13, Novosibirsk, USSR.
- [6] Dagenhart, J. R., Saric, W. S. (1999), Crossflow Stability and Transition Experiments in Swept-Wing Flow, NASA/TP-1999-209344
- [7] Mai H. and Hebler A. (2011). Aeroelasticity of a laminar wing, *IFASD 2011*, 26-30 June, Paris, France.
- [8] Lee T., Basu S. (1998), Measurement of unsteady boundary layer developed on an oscillating airfoil using multiple hot-film sensors, *Experiments in Fluids*, 25, 108-117
- [9] Rudmin D., Benaissa A., Poirel D. (2013). Detection of Laminar Flow Separation and Transition on a NACA-0012 Airfoil Using Surface Hot-Films, *Journal of Fluids Engineering*, 135.
- [10] Richter K., et al.(2012), Experimental Investigation of Unsteady Transition on a Pitching Rotor Blade Airfoil, *38<sup>th</sup> European Rotorcraft Forum*, 4-7 September 2012, Amsterdam, Netherlands
- [11] Studer G., Arnal D., Houdeville R. and Seraudie A. (2006). Laminar-turbulent transition in oscillating boundary layer: experimental and numerical analysis using continuous wavelet transform, *Experiments in Fluids*, 41:685-698.
- [12] Schmitt V. and Manie F. (1979). Ecoulements subsoniques et transsoniques sur une aile à fleche variable, *La Recherche Aéronautique*, 4:219-237
- [13] Arnal D., Coustols E., Juillen J.C. (1984). Etude expérimentale et théorique de la transition sur une aile en flèche infinie, *La Recherche Aéronautique*, 4, 275-290.
- [14] Arnal D., Juillen J.C. (1987), Three-Dimensional Transition Studies at ONERA/CERT, AIAA Conference, 19<sup>th</sup> Fluid Dynamics, Plasma Dynamics and Lasers Conference, 8-10 June, Honolulu, Hawaii.
- [15] Liauzun et al. (2019). Assessment of CFD methods taking into account laminar-turbulent transition for aeroelasticity of laminar wings, *IFASD 2019*, 9-13 June 2019, Savannah, Georgia, USA.
- [16] Perraud J., Deniau H., Casalis G. (2014). Overview of transition prediction tools in the elsA software, *ECCOMAS 2014*, July 2014, Barcelona, Spain.

## **COPYRIGHT STATEMENT**

The authors confirm that they, and/or their company or organization, hold copyright on all of the original material included in this paper. The authors also confirm that they have obtained permission, from the copyright holder of any third party material included in this paper, to publish it as part of their paper. The authors confirm that they give permission, or have obtained permission from the copyright holder of this paper, for the publication and distribution of this paper as part of the IFASD-2019 proceedings or as individual off-prints from the proceedings.